Fatigue & Fracture of
Engineering Materials & Structures

doi: 10.1111/j.1460-2695.2008.01263.x

A parametric study on fatigue strength of spot-weld joints

AHMET H. ERTAS and FAZIL O. SONMEZ

Department of Mechanical Engineering, Bogazici University, Istanbul, Bebek, 34342, Turkiye

Received in final form 15 July 2008

ABSTRACT Fastening elements usually lead to high stress concentrations; fatigue failure thus becomes the most critical failure mode for a fastening element itself or the region around it under fluctuating stresses. A designer should seek the ways of increasing fatigue strength of a joint to ensure the safety of the whole structure.

Resistance spot welding is the most preferred method to join metal sheets. The design variables for spot-weld joints affecting their strengths are basically sheet thickness, spot-weld nugget diameter, number of spot welds and the joint type as exemplified in tensile shear (TS), modified tensile shear (MTS), coach peel (CP) and modified coach peel (MCP) specimens.

In this study, the effects of these parameters on the fatigue life of spot-weld joints have been investigated. For this purpose, one of the most reliable fatigue assessment models, Coffin–Manson approach, was used. In order to accurately determine the stress and strain states, a nonlinear finite element analysis was carried out taking into account plastic deformations, residual stresses developed after unloading and contacting surfaces. The results provide designers with some guidelines to foresee the impact of design changes on fatigue strength of spot-weld joints.

Keywords fatigue life prediction; finite element analysis; plastic deformation; spot weld.

INTRODUCTION

In automotive, aerospace, railroad and many other applications, mechanical members usually experience cyclic loading. For this reason, they are liable to fail due to a fatigue fracture. Fatigue failure prevention then becomes the foremost design requirement for these parts. In knowing that fatigue crack initiation is very sensitive to stress level in that an increase in stress level dramatically increases the likelihood of fatigue failure, designers may significantly increase fatigue strength of a component by introducing changes in its geometry that reduces the level of stress in highly stressed regions. Spot welds like other joining elements induce very high stress concentration. By properly designing a spot-weld joint, one may reduce stress concentration, which will result in an increase in its fatigue life. In order to achieve a proper design for a spot-weld joint, one should know the effects of design variables on its fatigue life.

In the literature, the effects of spot-weld diameter,[1–7] number of spot welds,[3,4,8–10] metal sheet thickness,[1,4,5,9,11–13] metal sheet width,[1,5,6,13] joint type[2,3,5–7,11–15] and material[3,4,7,12,15–17] have been investigated using various experimental, theoretical, or numerical approaches. In this study, a more comprehensive objective is pursued, which is to determine the effects of sheet thickness, nugget diameter, number of spots and the joint type on the fatigue life of spot-weld joints. It should be noted that, as in any other design process, the design variables for spot welds are subject to some constraints, e.g. technological limits, difficulties in manufacturing, availability and cost. The range of values chosen in this study for the design variables is considered to be within the feasible range.

In order to determine the effects of the design variables accurately, first one should be able to determine the stress and strain states developed during the cyclic loading correctly. Plates that are joined by spot welds are subject to uniaxial in-plane loads, which means that even then multiaxial stresses will develop around the spot welds. Due to the high stress concentration, nonlinear deformation is likely to occur around the spots even at low loads. These stresses control the fatigue life of the joint and therefore the whole

Correspondence: Fazil O. Sonmez. E-mail: sonmezfa@boun.edu.tr

structure. For a reliable fatigue life assessment, one is required to determine, first of all, the stress field around the spot weld accurately. In this study, a nonlinear finite element analysis was carried out using nonlinear material properties and contact elements on the inner surfaces of the plates to find the stress and strain states. Plastic deformations and residual stresses developed after unloading were taken into account.

Second, one should use a reliable fatigue assessment model. In a previous study,[18] the predictions of many general purpose stress-based and strain-based fatigue assessment models were compared with experimental data. Two of these models, Coffin–Manson and Morrow mean stress, were observed to yield the best predictions. Therefore, in this study, these two models were used to predict fatigue life of various spot-weld designs.

MODELS FOR FATIGUE LIFE PREDICTION

Quite a number of models for fatigue life assessment have been proposed in the literature. They are classified either as strain-based or stress-based approaches in general. The predictions of stress-based approaches were found to be overly conservative for spot-weld joints,[18] which might be due to highly localized plastic deformation around the nuggets. In this study, only two of the strain-based models that yielded the best correlation with the experimental results were used to estimate fatigue lives of spot-weld joints.

One of these models is the local notch strain approach (or the Coffin–Manson model), which relates alternating true elastic and plastic strains, $\Delta\varepsilon_e$ and $\Delta\varepsilon_p$, to fatigue life, and shows the number of cycles to failure (N_f), as

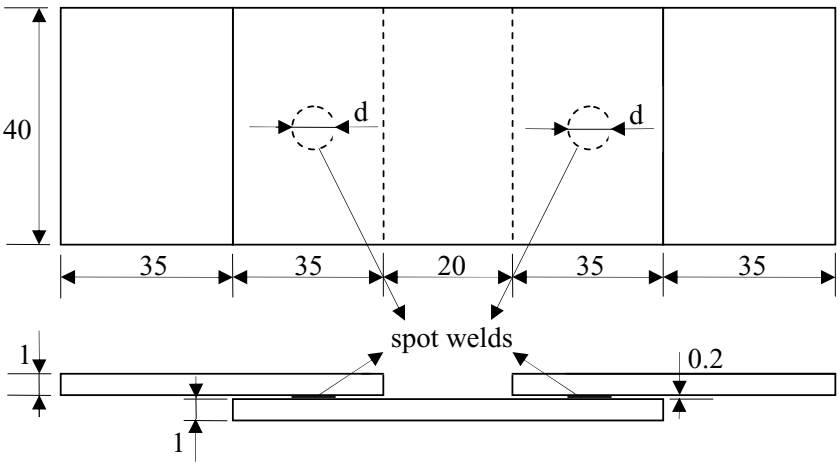

Fig. 1 Geometry of the tensile shear (TS) specimens (bottom and side views).

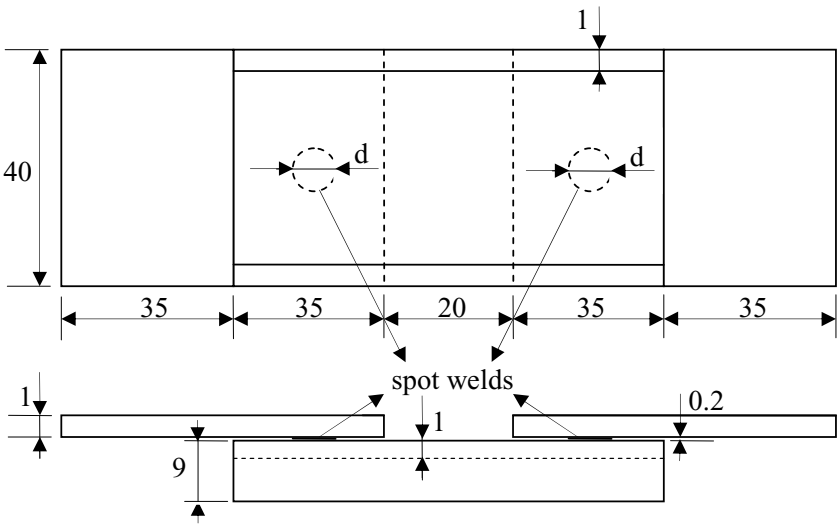

Fig. 2 Geometry of the modified tensile shear (MTS) specimens (bottom and side views).

follows[19,20]

$$\frac{\Delta\varepsilon}{2} = \frac{\Delta\varepsilon_e}{2} + \frac{\Delta\varepsilon_p}{2} = \frac{\sigma'_f}{E}\left(2N_f\right)^b + \varepsilon'_f\left(2N_f\right)^c, \quad (1)$$

where σ'_f is the fatigue strength coefficient, ε'_f is the fatigue ductility coefficient and b and c are exponents determined by experiments. The other one is the Morrow mean stress model, which includes the effect of mean stress on fatigue life by replacing σ'_f by $\sigma'_f - \sigma_m$ in Eq. (1), where σ_m is the mean stress:[19–21]

$$\frac{\Delta\varepsilon}{2} = \varepsilon_a = \frac{\Delta\varepsilon_e}{2} + \frac{\Delta\varepsilon_p}{2} = \frac{\sigma'_f - \sigma_m}{E}\left(2N_f\right)^b + \varepsilon'_f\left(2N_f\right)^c, \quad (2)$$

In the case of multiaxial stress and strain state, an equivalent uniaxial alternating strain, ε_{qa}, is calculated[19,20,22] which leads to the same fatigue life. In a previous study[18] octahedral shear strain was found to better clearly the effect of multiaxial strain state around the spot welds,

$$\varepsilon_{qa} = \frac{\sqrt{(\varepsilon_{a1} - \varepsilon_{a2})^2 + (\varepsilon_{a2} - \varepsilon_{a3})^2 + (\varepsilon_{a3} - \varepsilon_{a1})^2}}{\sqrt{2}\,(1 + \nu)}, \quad (3)$$

where $\varepsilon_{a1}, \varepsilon_{a2}$ and ε_{a3} are principal alternating strains with $\varepsilon_{a1} \rangle \varepsilon_{a2} \rangle \varepsilon_{a3}$.

GEOMETRY OF THE SPOT-WELD JOINTS

In this study, four commonly used joint types, tensile-shear (TS) modified tensile-shear (MTS), coach peel (CP) and modified coach peel (MCP), were considered. TS and MTS are made up of three strips of sheets joined by two spot welds as shown in Figs 1 and 2. Unlike TS specimens, MTS specimens contain plates bent at their sides. This increases the flexural rigidity, and thus resistance to bending and buckling. CP and MCP joints are made of two strips of sheets joined by one spot weld as shown in Figs 3 and 4. Because automated-type spot welds are formed by pressing the plates at both sides, some of the molten material is squeezed out into the interface between the plates. The extent of the slag material pushed into the interface between the plates may reach up to 10–20% of the sheet thickness.[18,29] In order to be on the conservative side, the space or gap between the overlapping portions of the plates was taken as 0.2 mm.

MATERIAL PROPERTIES

In the FE model, the material properties of St 12 03 (DIN 1623), a low carbon steel, were used. The engineering stress–strain diagram is given in Fig. 5. The elastic

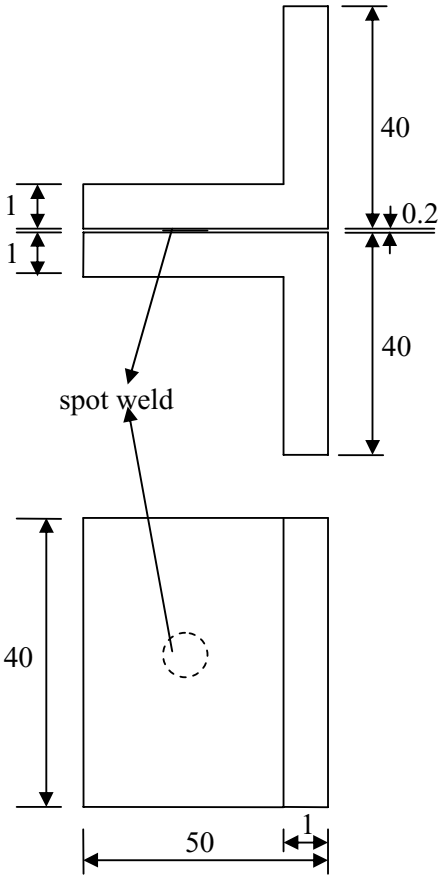

Fig. 3 Geometry of the coach peel (CP) specimens (side and top views).

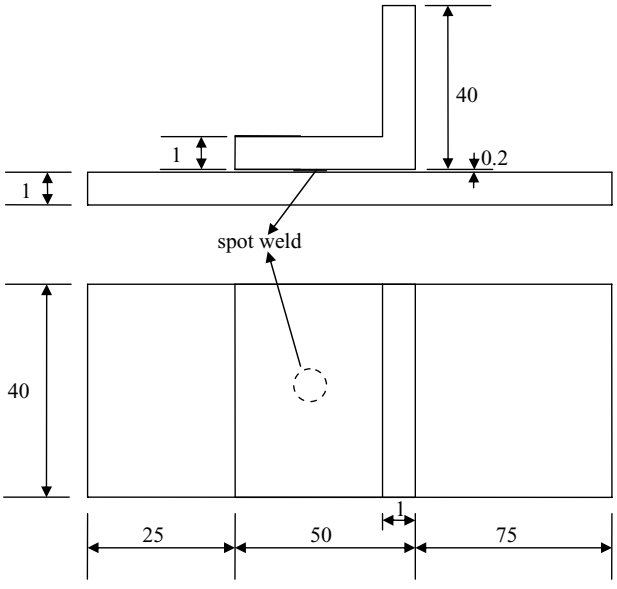

Fig. 4 Geometry of the modified coach peel (MCP) specimens (side and top views).

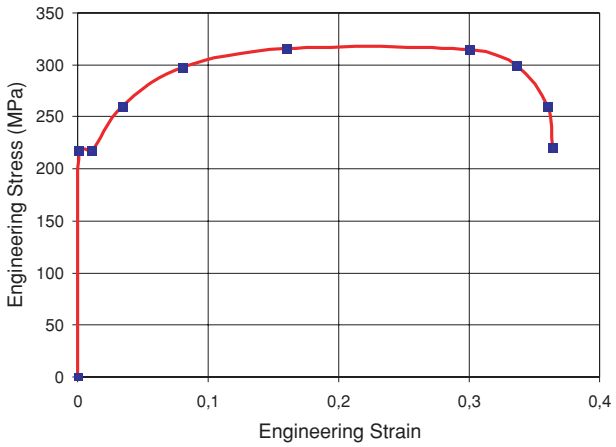

Fig. 5 Engineering stress–strain curve.[18]

properties of the material are $E = 207$ GPa, and $\nu = 0.25$[18] and the fatigue parameters are $\sigma'_f = 499$ MPa, $\varepsilon'_f = 0.104$, $b = -0.1$ and $c = -0.4$.[19] As heat treatment does not cause an appreciable change in elastic modulus and Poisson's ratio, it can be accepted that their magnitudes remain about the same throughout the specimen despite melting during the formation of the nugget. Though the fatigue parameters and the nonlinear stress–strain relation of the material in and around the nugget are affected during the joining operation, this effect was neglected considering that the steel was not hardened and heat treated.

FINITE ELEMENT MODEL

In order to employ fatigue life prediction models, the stress and strain states developed in the structure should be determined accurately. For this purpose, a commercial FEA software, ANSYS (version 10), was used. Residual stresses developed during the formation of the spot weld were not considered in the stress analysis. However, the residual stresses arising from non-uniform plastic deformations during loading were determined throughout the nonlinear stress analysis.

A kinematic hardening material model (KINH) was used to simulate the nonlinear stress–strain relation. This model includes the Besseling formulation, which takes into account the Bauschinger effect in cyclic loading. The data points were taken from the true stress–strain diagram obtained by converting the engineering stress–strain curve given in Fig. 5.

In the FE model, a 3D 10-node tetrahedral solid element, SOLID92, was used for the base metal. This element has plasticity, stress stiffening, large deflection and large strain capabilities. Several types of models have been proposed in the literature for spot-weld nuggets:

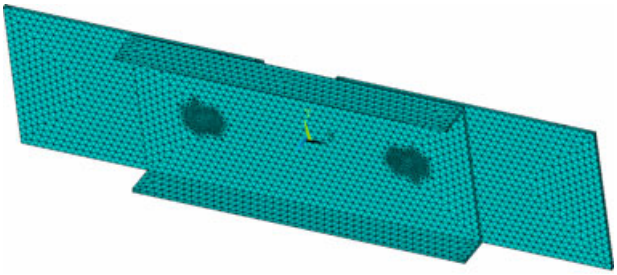

Fig. 6 Finite element model for the MTS specimen.

single-bar model,[23] spoke-bar model,[23,24] multiple rigid-bar model[23,25] and solid nugget model.[11,17,21,23,26–28] In this study, the nugget was modelled using a two-node beam element, BEAM188. The length of the beam element is taken the same as that of the gap, which is 0.2 mm. Contact and target elements, Targe170 and Conta175, were created on the inner surfaces around the spots. The radius of the contact region was chosen as four times the spot-weld radius. The beam element, BEAM188, is based on the Timoshenko beam theory. Shear deformation effects are therefore included, which are especially important for short beams. This element has six degrees of freedom at each node. One should note that the solid elements that are used to model the plates do not have rotational degrees of freedom unlike the beam element used for the nugget. In order to prevent relative rotation of plates with respect to spot weld at the connection points, the nodes on the plates that lie within the region of the spot-weld radius are constrained using the software capabilities. Considering that the nugget experiences low stresses, its material model was chosen as linearly elastic.

Due to high stress concentration, much smaller elements were used within and around the spot-weld nuggets in comparison to that of the base metal as shown in Fig. 6. The mesh density was also checked to ensure the convergence of stress values.

In ANSYS, a load step is applied in increments with a certain number of substeps. A convergence analysis was also performed to determine the number of substeps necessary for accuracy. Convergence was obtained in 160 substeps.

BOUNDARY CONDITIONS

The boundary conditions in the FE model of TS specimen are shown in Fig. 7. Displacements and rotations in all degrees of freedom are fixed at one end. The other end is subject to uniformly distributed in-plane load cycle in the x-direction, while the movement is prevented in the other degrees of freedom. The boundary

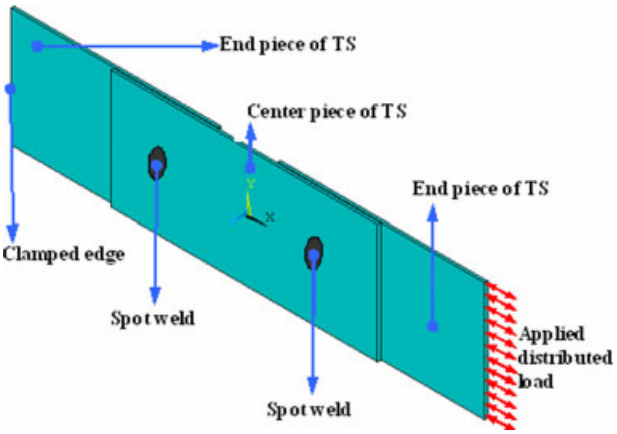

Fig. 7 Boundary conditions of the finite element model of TS.

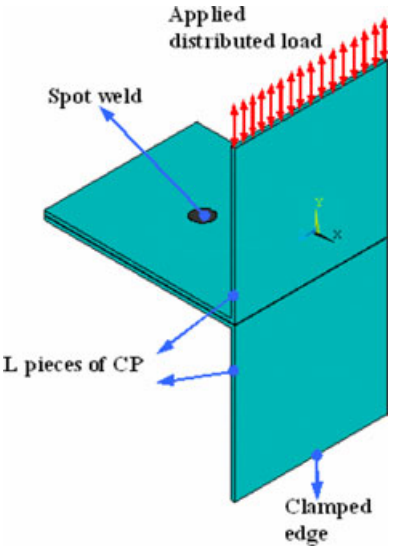

Fig. 8 Boundary conditions of the finite element model of CP.

conditions for MTS specimen are the same. The boundary conditions for CP and MCP are shown in Figs 8 and 9, respectively.

The cyclic loading was applied in two load steps. First, the load was incrementally increased to its maximum value, F_{max}, and the resulting stress state was obtained. In the second load step, the load was incrementally decreased to its minimum value, F_{min}. In the next load cycles, stresses were assumed to fluctuate between the stress values obtained for the maximum and minimum load levels in the first load cycle.

RESULTING STRESS STATES

Figures 10–13 show the distributions of the σ_{xx} component of stress on the inner and outer surfaces of the central pieces of TS and MTS, with specimens developing after

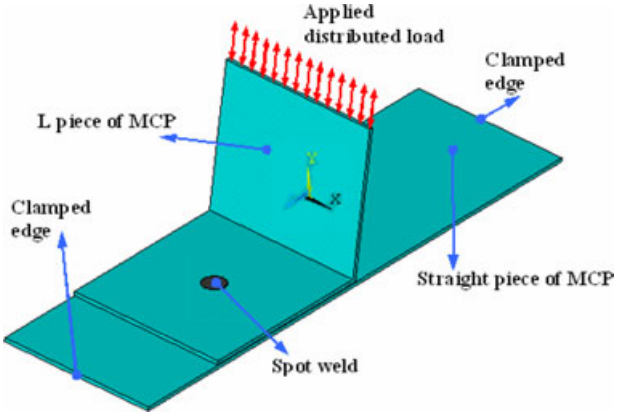

Fig. 9 Boundary conditions of the finite element model of MCP.

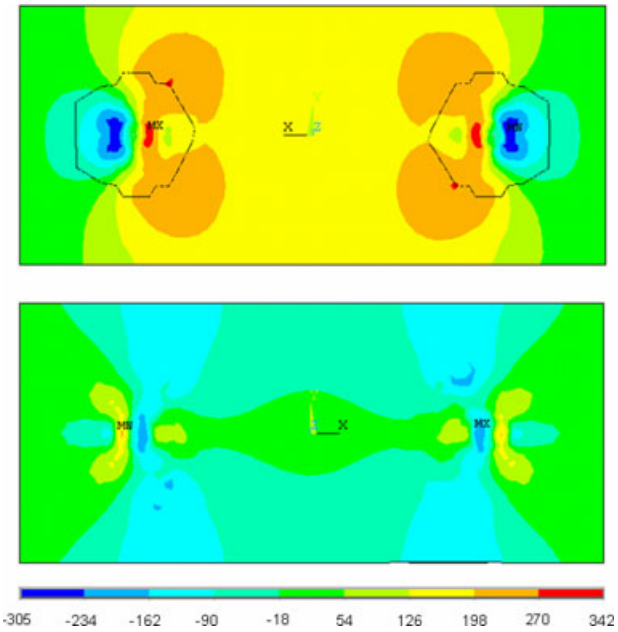

Fig. 10 Distribution of σ_{xx} component of true stress (in MPa) on the inner and outer surfaces of the central plate of a TS specimen developed due to the maximum load. ($t = 1$ mm, $d = 4$ mm, number of spots = 2).

the maximum (2700 N) and minimum (150 N) loads are applied. High stresses develop on the inner surfaces of the sheets close to the peripheries of the spot-weld nuggets. The peak tensile stress develops close to the spot weld but not on its circumference. The location of the high stress conforms to the fatigue crack initiation sites experimentally observed in previous studies.[18,21,29,30]

Because the minimum load is tensile and quite low (150 N), significant compressive stresses existing after unloading may only be attributed to residual stresses developed due to non-uniform plastic deformation. Although load transfer occurs through the spot-weld joint,

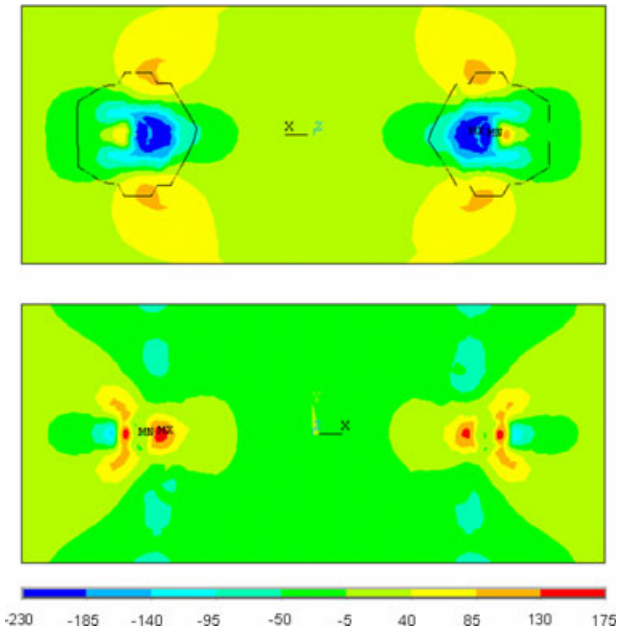

Fig. 11 Distribution of σ_{xx} component of true stress (in MPa) on the inner and outer surfaces of the central plate of a TS specimen developed due to the minimum load. ($t = 1$ mm, $d = 4$ mm, number of spots = 2).

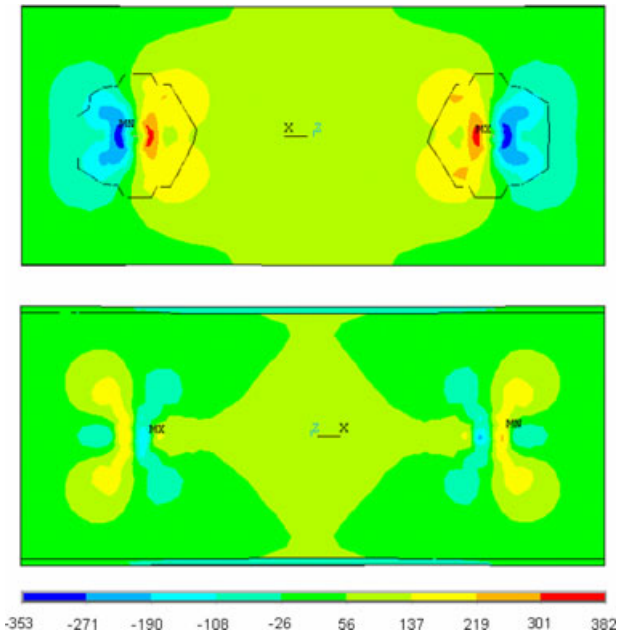

Fig. 12 Distribution of σ_{xx} component of true stress (in MPa) on the inner and outer surfaces of the central plate of a MTS specimen developed due to the maximum load. ($t = 1$ mm, $d = 4$ mm, number of spots = 2).

the nugget is subject to low stresses because its thickness is large in comparison to the sheet thickness. Besides which, the nugget is mainly subject to shear loading and the plate is mainly subject to bending moment. Consequently, bending induces larger stresses. Due to the effect of bending, stresses change from tension to compression through the thickness as seen in Figs 10 and 12. For this reason, flexural rigidity of the plate, i.e. its resistance to bending significantly affects the stress level even though the plates are subject to in-plane loading. The flanges of MTS specimens increase its flexural rigidity, especially at the sides. Considering that the load is transferred through the middle region, one may see why stresses are more concentrated in the MTS specimen (Fig. 12) in comparison to the TS specimen (Fig. 10). However, the peak compressive residual stress in the minimum load case is larger for the TS.

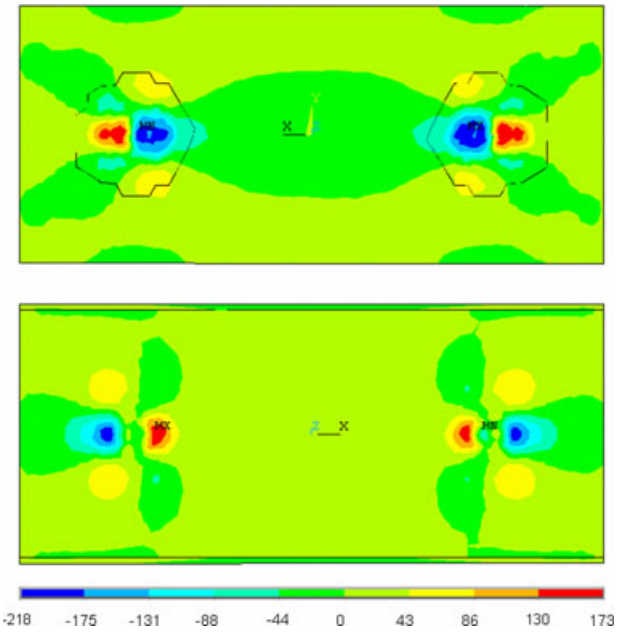

Fig. 13 Distribution of σ_{xx} component of true stress (in MPa) on the inner and outer surfaces of the central plate of a MTS specimen developed due to the minimum load ($t = 1$ mm, $d = 4$ mm, number of spots = 2).

Figures 14 and 15 show the effect of nugget diameter on stress distribution after the maximum load (2700 N) is applied. If the diameter is reduced to 2 mm, the stresses become extremely concentrated. In the case of 6-mm diameter, stress concentration is relieved and the maximum stress is reduced.

Figure 16 shows the stress distribution on the inner surface of TS specimens with 2-mm plate thickness after the maximum (2700 N) load is applied. Comparing with the stress distribution for 1 mm given in Fig. 10, one may see that the increase in thickness leads to a higher stress concentration, but a lower value for the highest stress. The reason for the more localized stress distribution may be attributed to the increased stiffness. Considering that

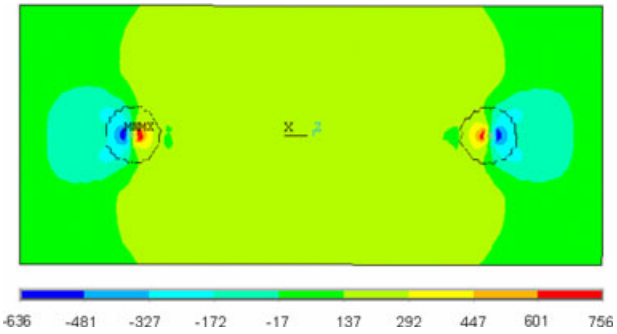

Fig. 14 Distribution of σ_{xx} component of true stress (in MPa) on the inner surface of the central plate of a TS specimen developed due to the maximum load. ($t = 1$ mm, $d = 2$ mm, number of spots = 2).

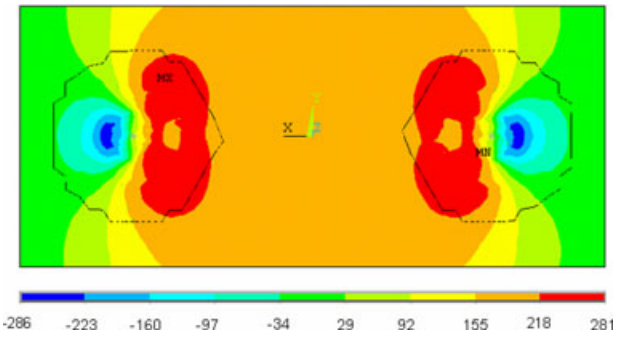

Fig. 15 Distribution of σ_{xx} component of true stress (in MPa) on the inner surface of the central plate of a TS specimen developed due to the maximum load. ($t = 1$ mm, $d = 6$ mm, number of spots = 2).

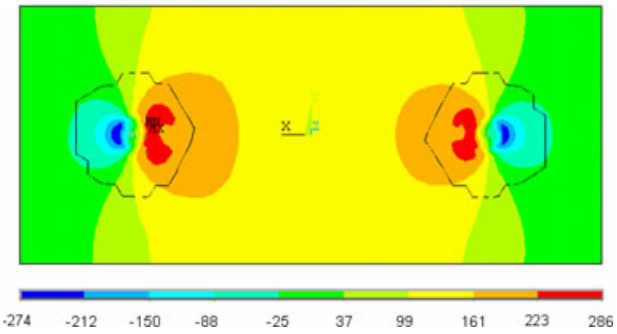

Fig. 16 Distribution of σ_{xx} component of true stress (in MPa) on the inner surface of the central plate of a TS specimen developed due to the maximum load. ($t = 2$ mm, $d = 4$ mm, number of spots = 2).

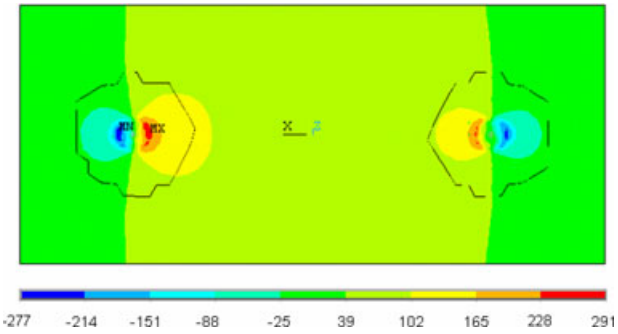

Fig. 17 Distribution of σ_{xx} component of true stress (in MPa) on the inner surface of the central plate of TS specimen developed due to the minimum load. ($t = 4$ mm, $d = 4$ mm, number of spots = 2).

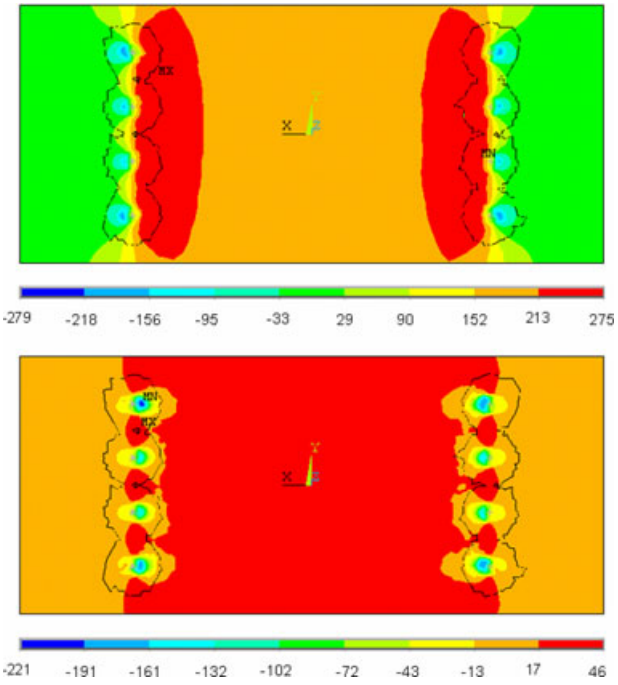

Fig. 18 Distribution of σ_{xx} component of true stress (in MPa) on the inner surface of the central plate of TS specimen developed due to the maximum and minimum load. ($t = 1$ mm, $d = 2$ mm, number of spots = 8).

a larger volume of material transfers the load, decrease in stress level is understandable. Increasing the thickness to 4 mm results in extremely high stress concentration as seen in Fig. 17. For this reason, decrease in stress level is not observed in this case.

Figure 18 shows the distributions of the σ_{xx} component of stress on the inner surface of central plate of a TS specimen developed after the maximum (2700 N) and minimum (150 N) loads are applied. This time, the plates are fastened using eight spots with 2-mm diameter, which have the same total cross-sectional as that of two spots with 4-mm diameter (Figs 10 and 11). For this case, stresses are uniformly distributed. Accordingly, residual stresses are reduced.

ESTIMATED FATIGUE LIVES

Calculation of fatigue lives

In a mechanical component under fluctuating loads, the process of nucleation, growth and joining of micro-cracks is expected to take place in highly stressed regions. Fatigue crack growth is known to occur along planes where the tensile stress takes its maximum value. Accordingly, the fatigue life calculations were carried out using the stress and strain states in the element at which the maximum tensile stress develops. This element is located at the faying surface around the peripheries of the spot welds as shown in Figs 10–13.

Comparison of the predicted and measured fatigue lives

The accuracy of the fatigue life predictions was verified by comparing them with the fatigue lives of MCP and MTS specimens experimentally obtained by Pan[21] and Ertas *et al.*[18] The FE calculations were carried out using the material properties, loading and geometry of the specimens provided in those studies. Fatigue lives were predicted using Coffin–Manson and Morrow's mean stress models. As seen in Figs 19–21, the results compare quite well. Correlation of Coffin–Manson model with the experimental data is better. It should also be noted that better correlation obtained with the data provided by Pan[21] in comparison to the data provided by Ertas *et al.*[18] may be attributed to the use of the material properties of HAZ in the former case rather than the properties of base metal in the other case.

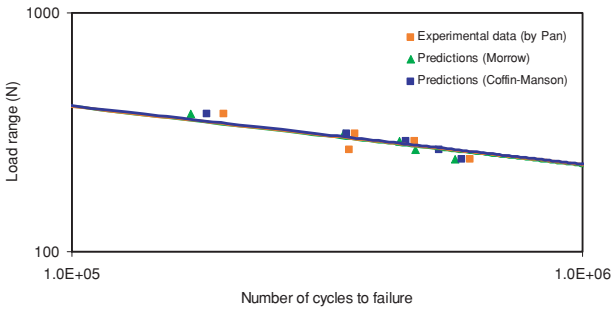

Fig. 19 Comparison of predicted fatigue lives with experimental results obtained by Pan (for DQSK MCP specimens).[21]

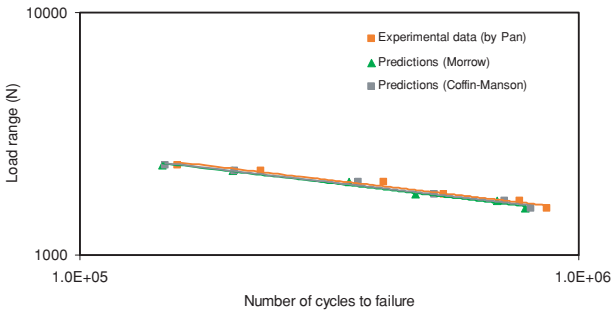

Fig. 20 Comparison of predicted fatigue lives with experimental results obtained by Pan (for DQSK MTS specimens).[21]

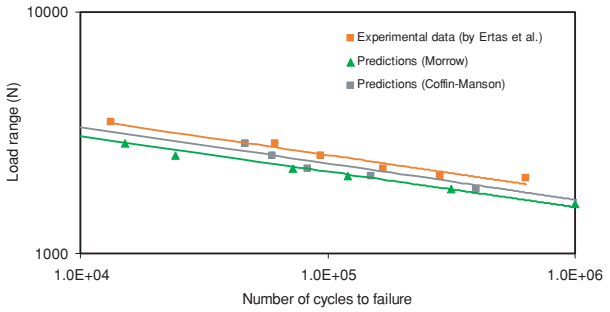

Fig. 21 Comparison of predicted fatigue lives with experimental results obtained by Ertas *et al.* (for DIN 1623 MTS specimens).[18,29]

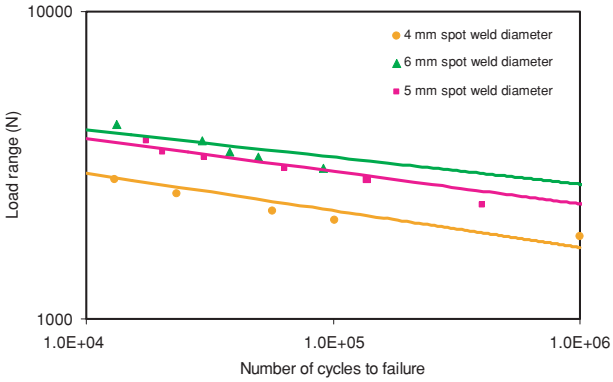

Fig. 22 Fatigue lives predicted using Coffin–Manson approach for TS specimens with 1-mm thickness and different spot-weld diameters.

Results and discussions

A parametric study was conducted to determine the effects of design variables on fatigue life. The basic geometry was chosen as a TS specimen with 4-mm diameter spot weld and 1-mm thick sheet. In order to see the effects of a variable, only one variable is changed while the others are kept constant. Accordingly, fatigue lives of TS and MTS specimens with three different spot-weld diameters (4 mm, 5 mm, and 6 mm) and three different plate thicknesses (1 mm, 1.5 mm, and 2 mm) were calculated using Coffin–Manson model. Figures 22–25 present the results. As shown in Fig. 22, joints with larger spot-weld diameters have much higher fatigue strength. This is because a larger region transmits the applied load, which reduces stress concentration as indicated in Figs 14 and 15. The

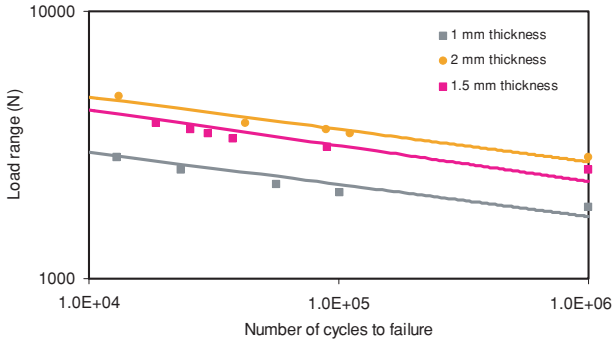

Fig. 23 Fatigue lives predicted using Coffin–Manson approach for TS specimens with 4-mm spot diameter and different metal sheet thicknesses.

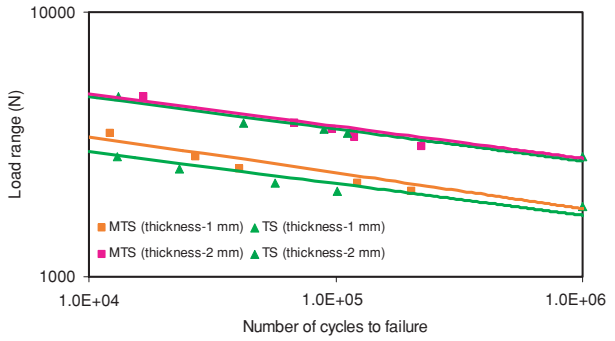

Fig. 24 Comparison of fatigue lives calculated using Coffin–Manson approach for MTS and TS specimens with 4-mm spot diameter and different metal sheet thicknesses.

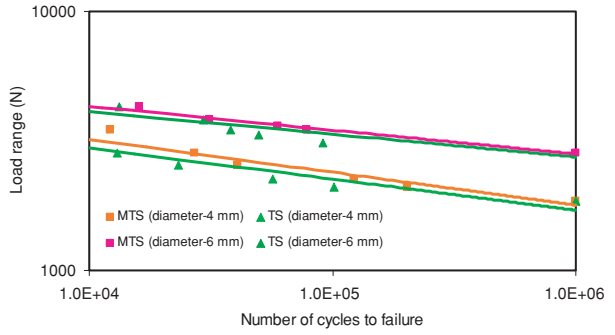

Fig. 25 Comparison of fatigue lives calculated using Coffin–Manson approach for MTS and TS specimens with 1-mm thickness and different spot-weld diameters.

improvement obtained by increasing the diameter from 5 mm to 6 mm is less pronounced.

As seen in Fig. 23, the fatigue strength is significantly improved when the thickness is increased from 1.0 mm to 1.5 mm due to the reduction in the maximum stress level as seen in Figs 10 and 16. However, there is a relatively small increase in fatigue strength when the thickness is increased from 1.5 mm to 2.0 mm. This means that this design change, which increases material cost and weight by 33%, does not considerably improve the performance of the joint.

Table 1 Comparison of the fatigue lives (number of cycles to failure) of different joint types ($t = 1$ mm and $d = 4$ mm)

	Load range		
Specimen type	2700N/150N	2250N/150N	2000N/150N
CP	2357	2704	13 053
MCP	29 663	181 200	192 184
TS	15 288	68 997	$>1 \times 10^6$
MTS	24 227	120 964	$>1 \times 10^6$

Figures 24 and 25 show a comparison of the fatigue behaviours of MTS and TS specimens for different sheet thicknesses and different spot-weld diameters, respectively. Although MTS specimen has a larger flexural strength, its fatigue strength is not greatly improved because this leads to a higher stress concentration. The fatigue strength of MTS is better for small thickness and diameters. For large diameters and thicknesses, they have comparable strengths. This may be due to the increased contribution of thickness to flexural rigidity in comparison to that of the flange of the MTS specimen.

Table 1 gives a comparison of fatigue lives of different joint types for different load ranges. CP provides the weakest connection among all; therefore it should be avoided if possible. CP may be used if the plates cannot be gripped from both sides due to space limitations. Even in that case, one may prefer a TS joint with manual spot welds because they are achieved by touching the electrode on one surface of the plate without applying force. MCP is weaker in comparison to TS and MTS for the load case of 2000N/150N. However, when the load is increased deterioration in fatigue life is less pronounced for MCP. This is because when the load is increased the yield zone expands, but the maximum stress slightly increases.

Tables 2 and 3 give fatigue lives of TS specimens connected by different numbers of spot welds having different diameters. As seen in Table 2, the joint with eight spots having 2-mm diameter is much stronger than that with

Table 2 Fatigue lives of TS specimens with different numbers and diameters of spots ($t = 1$ mm and $d = 4$ mm).

		Load range		
No. of spots	Diameter	5000N/200N	3700N/200N	3000N/150N
2	4 mm	3162	3930	8194
8	2 mm	4687	21 072	$>1 \times 10^6$

Table 3 Fatigue lives of TS specimens with different numbers and diameters of spots ($t = 1$ mm and $d = 5.66$ mm).

No. of spots	Diameter	Load range 4500N/200N	3700N/200N	3500N/200N
2	5.66 mm	5659	31 967	53 637
4	4 mm	5856	33 911	56 409

two spots having 4-mm diameter even though the total cross-sectional areas are the same. Similarly, the joint with four spots having 4-mm diameter is stronger than that with two spots having 5.66-mm diameter, which have the same total cross-sectional areas (Table 3). This implies that a joint with larger but fewer number of spots is weaker than a joint with smaller but larger number of spots. This means that instead of increasing the nugget diameter, it is better to increase the number of spots if the increase in manufacturing time can be tolerated.

CONCLUSIONS

In this study, the fatigue lives of TS, MTS, CP and MCP type spot-weld joints were estimated for various spot-weld diameters and sheet thicknesses using Coffin–Manson model.

Fatigue life of a spot-welded joint highly depends on the joint type, applied load amplitude, sheet thickness, and the spot-weld diameter. The resistance of TS to fatigue failure is slightly lower in comparison to MTS for small nugget diameters and thicknesses. For larger diameters and thicknesses, TS and MTS have about the same fatigue resistance. Larger flexural rigidity of MTS specimens does not conduce to great improvement in fatigue life because of a higher stress concentration. For this reason, one should not expect to improve fatigue strength by introducing flanges to plates fastened by spot welds except for better deformation behaviour. This will only increase material and manufacturing cost, and weight. Fatigue strength of CP joints is much lower in comparison to MCP, TS and MTS. Hence, one should avoid using CP joints under tensile fluctuating loads.

Larger diameters and thicknesses resulted in longer fatigue lives within the chosen range of values for these parameters. However, after a certain limit, increase in thickness does not improve fatigue strength. For this reason, one should find the optimum thickness through fatigue analyses in a design process for effective use of material. Moreover, using a larger number of small spot welds proved to be more effective in increasing fatigue strength in comparison to large spots having the same cross-sectional area.

Acknowledgements

This paper is based on the work supported by TUBITAK with the code number 106M301.

REFERENCES

1 Zhou, M., Hu, S. J. and Zhang, H. (1999) Critical specimen sizes for tensile-shear testing of steel sheets. *Weld. J.*, 305s–313s.
2 Barkey, M. E., Kang, H. and Lee, Y. (2000) Evaluation of multiaxial spot weld fatigue parameters for proportional loading. *Int. J. Fatigue.* **22**, 691–702.
3 Gean, A., Westgate, S. A., Kucza, J. C. and Ehrstrom, J. C. (1999) Static and fatigue behavior of spot-welded 5182-O aluminum alloy sheet. *Weld. J.* 90s–96s.
4 Davidson, J. A. (1983) A review of the fatigue properties of spot-welded sheet steels, Detroit Michigan. *Proceedings of the SAE The Engineering Resource for Advancing Mobility*.
5 Zhang, S. (1997) Stress intensities at spot welds. *Int. J. Fract.* **88**, 167–185.
6 Davidson, J. A. and Imhof, E. J. (1983) A fracture-mechanics and system-stiffness approach to fatigue performance of spot-welded sheet steels, Detroit Michigan. *Proceedings of the SAE The Engineering Resource for Advancing Mobility*.
7 Thornton, P. H., Krause, A. R. and Davies, R. G. (1996) The aluminum spot weld. *Weld. J.* 101s–108s.
8 Adib, H., Gilgert, J. and Pluvinage, G. (2004) Fatigue life duration prediction for welded spots by volumetric method. *Int J Fatigue*. **26**, 81–94.
9 Matsoukas, G., Steven, G. P. and Mai, Y. W. (1984) Fatigue of spot-welded lap joints. *Int. J. Fatigue.* **6**, 55–57.
10 Pook, L. P. (1975) Fracture mechanics analysis of the fatigue behaviour of spot welds. *Int. J. Fracture*. **11**, 173–176.
11 Pan, N. and Sheppard, S. (2002) Spot welds fatigue life prediction with cyclic strain range. *Int. J. Fatigue.* **24**, 519–528.
12 Pollard, B. (1982) Fatigue strength of spot welds in Titanium-bearing HSLA steels, Detroit Michigan. *Proceedings of the SAE The Engineering Resource For Advancing Mobility*.
13 Bae, D. H., Sohn, I. S. and Hong, J. K. (2003) Assessing the effects of residual stresses on the fatigue strength of spot welds. *Weld. J.* 18s–23s.
14 Wonseok, J., Dongho, B. and Ilseon, S. (2004) Fatigue design of various type spot welded lap joints using the maximum stress. *KSME Int. J.* **18**, 106–113.
15 Rathbun, R. W., Matlock, D. K. and Speer, J. G. (2003) Fatigue behavior of spot-welded high-strength sheet steels. *Weld. J.* 207s–218s.
16 Linder, J. and Melander, A. (1998) Fatigue strength of spot welded stainless sheet steels exposed to 3% NaCl solution. *Int. J. Fatigue* **20**, 383–388.
17 Newman, J. A. and Dowling, N. E. (1998). A crack growth approach to life prediction of spot-welded lap joints. *Fatigue Fract. Engng Mater. Struct.* **21**, 1123–1132.
18 Ertas, A. H., Vardar, O., Sonmez, F. O. and Solim, Z. Measurement and assessment of fatigue life of spot weld joints to appear in Transactions of ASME; Journal of Engineering Materials Technology.
19 Stephens, R. I., Fatemi, A., Stephens, R. R. and Fuchs, H. O. (2001) *Metal Fatigue in Engineering*. A Wiley-Interscience Publication, New York, USA.

20 Suresh, S. (2004) *Fatigue of Materials*. Cambridge University Press, Cambridge.
21 Pan, N. (2000) *Fatigue Life Study of Spot Welds*. Ph.D. Thesis Dissertation, Stanford University.
22 Schijve, J. (2001) *Fatigue of Structures and Materials*, A Kluwer Academic Publication, Dordrecht.
23 Xu, S. and Deng, X. (2004) An evaluation of simplified finite element models for spot welded joints. *Finite Elem. Anal. Des.* 40, 1175-1194.
24 Zhang, S. (2001) Approximate stress formulas for a multiaxial spot weld specimen. *Weld. J.* 201s–203s.
25 Hou, Z., Wang, Y., Li, C. and Chen, C. (2006) An analysis of resistance spot welding. *Weld. J.* 36s–40s.
26 Deng, X., Chen, W. and Shi, G. (2000) Three-dimensional finite element analysis of the mechanical behavior of spot welds. *Finite Elem. Anal. Des.* **35**, 17–39.
27 Chao, Y. J. (2003) Failure mode of spot welds: interfacial versus pullout. *Sci. Technol. Weld. Joi.* **8**, 133–137.
28 Salvini, P., Vivio, F. and Vullo, V. (2000) A spot weld finite element for structural modeling. *Int. J. Fatigue* **22**, 645–656.
29 Ertas, A. H. (2004) *Fatigue Behavior of Spot Welds*. M. Sc. Thesis Dissertation, Bogazici University.
30 Sheppard, S. D. and Strange, M. (1992) Fatigue life estimation in resistance spot welds: initiation and early growth phase. *Fatigue Fract. Engng Mater. Struct.* **15**, 531–549.